

# Crystal Structural Studies of Thermal Decomposition Process of $\text{PbMg}_{1/3}\text{Nb}_{2/3}\text{O}_3$ Single Crystal into Pyrochlore Type Compound

Naoki WAKIYA, Nobuo ISHIZAWA\*, Atsushi SAIKI, Kazuo SHINOZAKI and Nobuyasu MIZUTANI†

Department of Inorganic Materials, Faculty of Engineering, Tokyo Institute of Technology, 2-12-1, O-okayama, Meguro-ku, Tokyo 152

\*Research Laboratory of Engineering Materials, Tokyo Institute of Technology, 4295, Nagatsuta-cho, Midori-ku, Yokohama-shi, Kanagawa 227

## 結晶構造の観点から見た $\text{PbMg}_{1/3}\text{Nb}_{2/3}\text{O}_3$ のパイロクロア型化合物への熱分解挙動

脇谷尚樹・石沢伸夫\*・佐伯 淳・篠崎和夫・水谷惟恭

東京工業大学工学部無機材料工学科, 152 東京都目黒区大岡山 2-12-1

\*東京工業大学工業材料研究所, 227 神奈川県横浜市緑区長津田町 4259

[Received June 14, 1993; Accepted October 7, 1993]

Crystal structure parameters including *B* thermal parameters of each constituent atom were determined for  $\text{PbMg}_{1/3}\text{Nb}_{2/3}\text{O}_3$  (PMN) between 27 and 700°C by the single crystal high temperature X-ray diffraction technique. For lead, and magnesium and niobium atoms, the optimum shift directions from the special positions were not a single direction but "spherical" shifts were observed. For oxygen atom, it was confirmed that the optimum shift direction was not one ring on *XY* plane but two parallel rings away from *XY* plane. PMN began to decompose into polycrystalline pyrochlore type compound at 600°C. The mechanism of decomposition was discussed from the view point of crystal structure.

**Key-words** : Lead magnesium niobium oxide, PMN, Single crystal, Crystal structure determination, Pyrochlore, Thermal decomposition

### 1. Introduction

$\text{PbMg}_{1/3}\text{Nb}_{2/3}\text{O}_3$  (PMN) has been widely investigated from the view point of its high dielectric constant and diffuse phase transition (DPT).<sup>1)</sup> Mizutani et al.<sup>2)</sup> reported that PMN decomposed into pyrochlore type compound toward a bulk from a surface at high temperature with the evaporation of PbO and went back into the original PMN phase with the reaction with PbO under the controlled PbO atmosphere. Moreover Jang et al.<sup>3)</sup> reported that perovskite PZN decomposed into pyrochlore type compound by annealing a pure  $\text{PbZn}_{1/3}\text{Nb}_{2/3}\text{O}_3$  (PZN) specimen for 1h at various temperatures. However, the behaviors about the decomposition of perovskite into pyrochlore type compound at high temperature have not been discussed yet from the point of crystal structure view in these papers.

The crystal structure of PMN has been tried to determine by many investigators using HRTEM, powder X-ray and neutron diffraction techniques.<sup>4)-14)</sup> In these reports, the directions of disordered motions of

Pb, (Mg, Nb) and O atoms from the special crystallographic sites of the ideal cubic perovskite structure<sup>15)</sup> have been discussed in the wide temperature range. However, no structural correlations on the decomposition of perovskite PMN into pyrochlore type compound have been clarified yet. Therefore the purpose of this work is to investigate the structural correlations using PMN single crystal in the temperature range between 27 and 700°C.

### 2. Experimental

#### 2.1 Preparation of single crystal

In order to grow PMN single crystal, the pseudo-binary PMN-PbO phase diagram<sup>16)</sup> was referred. The growth condition was the same as our previous report<sup>17)</sup> except for the cooling rate of 1°C/h. The chemical analysis data of grown single crystal were shown in Table 1. The cation ratio was analyzed by ICP-AES (Seiko Instruments, SPS-1500 VR). The oxygen content was measured by LECO's oxygen analyzer (LECO, TC-436).

#### 2.2 Data collection and refinements

The grown crystal was shaped into a sphere of 0.12 mm diameter for the high-temperature X-ray study. The crystal was mounted on a quartz glass capillary with  $\text{ZrSiO}_4$  cement. A four-circle diffractometer (Philips, PW1100) equipped with a small specimen heating unit<sup>18)</sup> was used for the determination of the lattice parameter and the collection of in-

Table 1. Chemical Analysis Data

ICP-AES (Cation Ratio)		LECO (Oxygen Content)	
Sample Weight 52mg		Sample Weight 3.0mg	
Pb	73.8 ± 0.6wt%	O	14.6 ± 0.09wt%
Mg	2.83 ± 0.02wt%		
Nb	23.4 ± 0.12wt%		
Analytical Composition $\text{Pb}_{0.97}\text{Mg}_{0.32}\text{Nb}_{0.68}\text{O}_3$			

† To whom correspondence should be addressed.

tensity data between 27 and 700°C. The specimen was heated in a hot air stream. The temperature of the specimen was measured with a 0.08 mm Pt-PtRh13% thermocouple placed at a point about 0.1 mm away from the specimen and was kept constant within  $\pm 5^\circ\text{C}$  during the measurements. Lattice parameter at each temperature was calculated from the 6 reflections in the range  $3.5 < \theta < 23^\circ$  (Mo  $K\alpha$ ) using the program RLC-3.<sup>19)</sup> Intensities were collected with Mo  $K\alpha$  radiation monochromatized with a graphite plate. The  $\omega$ - $2\theta$  scan technique was employed with scanning speeds of  $4^\circ/\text{min}$  in  $\omega$ , and scanning was repeated up to three times when the total counts were less than 10000. The scanning width was  $2.0^\circ$ . Independent reflection data that satisfied the relation  $|F_0| > 3\sigma|F_0|$  were used in the subsequent refinement. Intensities were corrected for Lorentz, polarization and absorption factors. Extinction corrections were made in the course of the refinement. The structure was refined with the full-matrix least-squares program LINUS.<sup>20)</sup> The atomic scattering factors for  $\text{Pb}^{2+}$ ,  $\text{Mg}^{2+}$  and  $\text{Nb}^{5+}$  were referred to International Tables for X-ray Crystallography (1974) and that of  $\text{O}^{2-}$  was referred to Tokonami.<sup>21)</sup>

### 3. Results

Figure 1 shows the change of integrated intensity of (110) peak with heating temperature. Because of the degradation of intensity by decomposition, the measurement of intensity was carried out after data collection at each temperature was finished. The intensity began to decrease at 600°C due to the decomposition of PMN single crystal.

On the crystal structure determination of PMN, the shift directions for each constituent atom from the special crystallographic sites have been frequently discussed,<sup>8),12),14)</sup> however, the shift directions proposed for each atom were not always same in these reports. For example the shift direction of Pb atom was reported to be  $\langle 110 \rangle$ ,<sup>8)</sup>  $\langle 110 \rangle$  or  $\langle 111 \rangle$ <sup>12)</sup>

and  $\langle 225 \rangle$ .<sup>14)</sup> To determine the shift directions of each constituent atom, the atomic positions were fixed in their special positions and the Fourier difference maps were calculated in the whole temperature range. The directions of residual electron around Pb and (Mg, Nb) atoms were not specified but spherical residual electrons were observed. In all previous<sup>8),12),14)</sup> reports, only one shift direction model for each atom has been discussed. However, the results of Fourier difference maps suggested that the direction of shifts was not so simple. Consequently, a new model about the shift directions of each constituent atom should be proposed in order to improve the accuracy of refinements. The new model was examined against the data collected at 27°C. At first, for Pb atom, the position was refined using simple  $\langle 100 \rangle$ ,  $\langle 110 \rangle$  and  $\langle 111 \rangle$  shift direction models and obtained 14.49, 11.85 and 13.44% of *R*-factors respectively. Secondly, a new model that was approximated by the spherical residual electron was examined. In this model, Pb site was divided into three sites with different shift directions from the special positions. That is, a third of Pb shifted to  $\langle 100 \rangle$  direction, next a third of Pb shifted to  $\langle 110 \rangle$  direction and the last a third of Pb shifted to  $\langle 111 \rangle$  direction. Hereafter this model was designated as  $\langle 100/110/111 \rangle$  shift direction model. With this model, the *R*-factor fell to 8.94%. If the model of spherical shift could be completed, the *R*-factor would be much improved. In the same way, the position of (Mg, Nb) atoms was examined. Consequently, as well as Pb atom, it was clarified that the  $\langle 100/110/111 \rangle$  shift direction model was also plausible for (Mg, Nb) atoms.

For the shift direction of O atom, two models have been proposed in the literatures, that is, two parallel rings away from the *XY* plane model<sup>12)</sup> and one ring on the *XY* plane model.<sup>14)</sup> In our refinements, both the two models were examined. Consequently, *R*-factor fell to 6.83 and 7.02% in the former and the latter models, respectively. From this result it was clarified that the former model was plausible. These shift directions of each constituent atom were examined in the temperature range between 27 and 700°C in the same way, and were found to be valid up to 700°C.

Taking these positions and reported *B* thermal parameters<sup>12)</sup> as starting parameters, the positions of each atom were refined by full-matrix least squares calculation thereafter *B* thermal parameters were refined by full-matrix least squares calculation. Change of displacements from the special positions for each constituent atom with temperature up to 700°C was shown in Fig. 2. The reported values of displacements<sup>8),12),14)</sup> were also plotted in Fig. 2 for comparison. Change of *B* thermal parameters for each constituent atom with temperature up to 700°C was shown in Fig. 3. The final *R*-factors were between 3.6 and 7.5% in the whole temperature range.

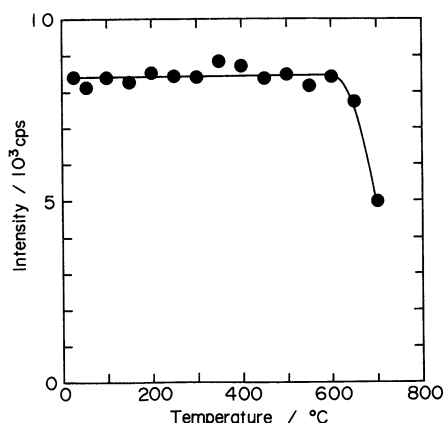


Fig. 1. Relationship between integrated intensity of (110) peak and temperature.

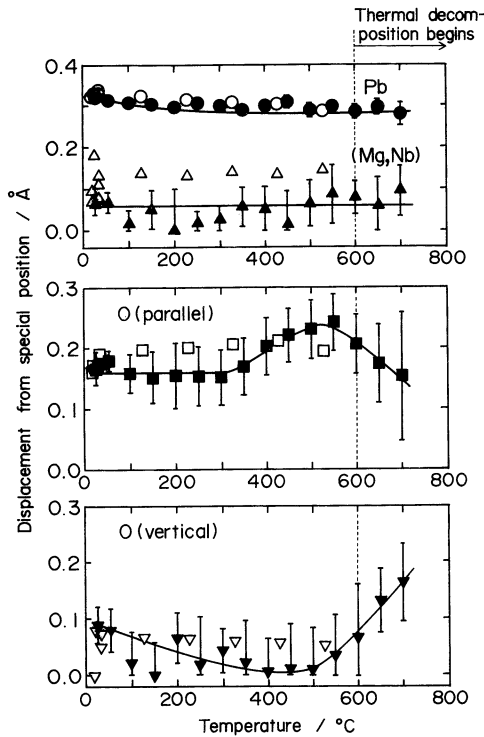


Fig. 2. Relationship between the displacements from the special positions of each constituent atom and temperature.  
 ●▲■▼ : This work, ○△□▽ : Reported values.

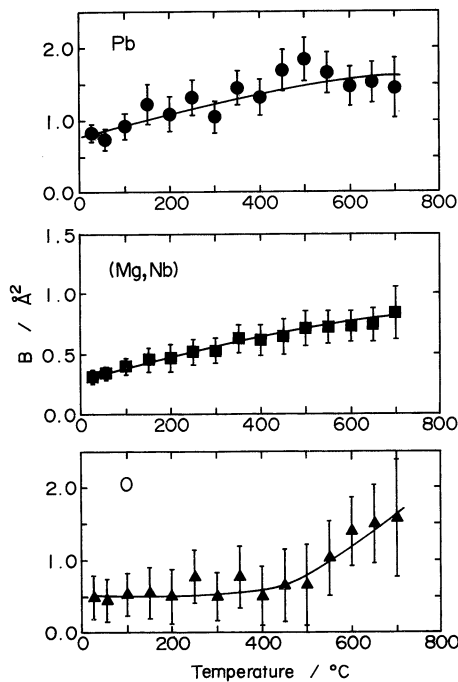


Fig. 3. Relationship between  $B$  thermal parameters of each constituent atom and temperature.

#### 4. Discussion

As mentioned above, the relationship between the change of displacements from the special positions for each constituent atom and temperature has been reported up to 800 K.<sup>8),12),14)</sup> Comparing these data

with our results (Fig. 2), the values of displacements from the special position of each constituent atom were almost identical within the error bars under 600°C in spite of the different shift direction models (spherical shift model for Pb and (Mg, Nb) atoms was adopted in our refinements). The purpose of this investigation is to clarify the structural correlation about the decomposition of perovskite PMN into pyrochlore type compound at high temperature. From Fig. 1, it was clarified that PMN began to decompose at 600°C. Therefore the data above 600°C in Fig. 2 indicate the change of displacements when PMN thermally decomposed into pyrochlore type compound. For Pb and (Mg, Nb) atoms, the magnitude of displacements from the special positions above 600°C was almost identical to that below 600°C. On the other hand, for O atom vertical to  $XY$  plane, the magnitude of displacement from the special position drastically increased above 600°C. Figure 4(a) shows an ideal linkage of (Mg, Nb) $\text{O}_6$  octahedra in PMN along  $\langle 100 \rangle$  direction. Because of the displacements of (Mg, Nb) and O atoms from the special positions, there exist long and short (Mg, Nb)–O distances locally as shown in Fig. 4(b) even at room temperature. According to Hazen and Prewitt,<sup>22)</sup> mean coefficient of linear thermal expansion from 23 to 1000°C is  $14.3 \times 10^{-6}/^\circ\text{C}$  while 0/°C for  $\text{Mg}^{2+}\text{--O}$  and  $\text{Nb}^{5+}\text{--O}$  distances, respectively. Considering this difference of linear thermal expansion

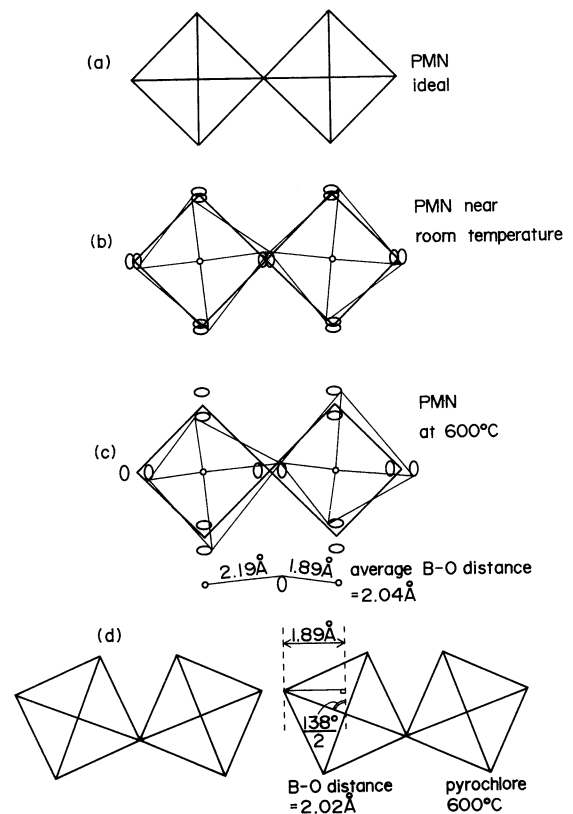


Fig. 4. Schematic figure of  $\text{BO}_6$  octahedra linkage.  
 (a) PMN ideal, (b) PMN near room temperature, (c) PMN at 600°C, (d) pyrochlore type compound at 600°C.

sion coefficients, the difference between long and short (Mg, Nb)-O distances are magnified at high temperature. Figure 5 shows the change of short (Mg, Nb)-O distance with temperature. From this figure, it was clarified that the short (Mg, Nb)-O distance actually began to decrease above 500°C. Figures 6(a) and (b) shows arrangement of  $\text{BO}_6$  octahedra in the perovskite and pyrochlore structure, respectively. As shown in this figure, B-O-B angle along  $\langle 100 \rangle$  direction in the perovskite structure is  $180^\circ$ , while that along  $\langle 110 \rangle$  direction in the pyrochlore structure is around  $138^\circ$ , therefore the  $\text{BO}_6$  octahedra link in zig-zag line. Figure 4(c) shows a schematic figure of  $\text{BO}_6$  octahedra linkage in PMN at  $600^\circ\text{C}$ . At this temperature the short (Mg, Nb)-O distance is  $1.89 \text{ \AA}$ . Figure 4(d) shows schematic figure of  $\text{BO}_6$  octahedra linkage in the pyrochlore type compound at  $600^\circ\text{C}$ . The B-O distance determined from the structure refinement using pyrochlore single crystal<sup>17)</sup> at this temperature was  $2.02 \text{ \AA}$ . Because of the similarity between the perovskite and pyrochlore shown in Fig. 6, the or-

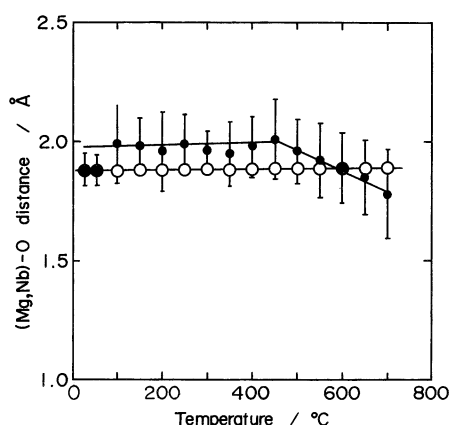


Fig. 5. Change of short (Mg, Nb)-O distance in PMN (●) and the orthogonal projection of (Mg, Nb)-O distance along  $\langle 110 \rangle$  direction of pyrochlore type compound (○) with temperature.

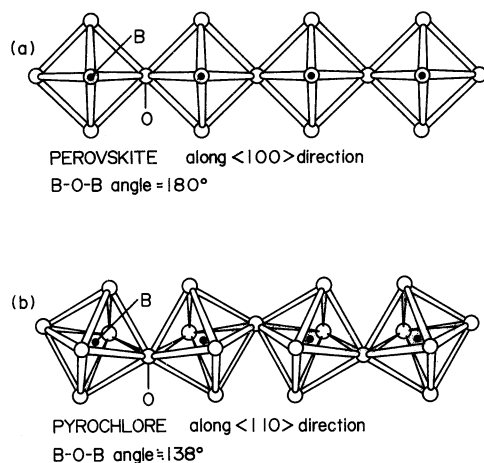


Fig. 6. Arrangement of  $\text{BO}_6$  octahedra in the perovskite and pyrochlore structure.

thogonal projection of B-O distance of pyrochlore on  $\langle 110 \rangle$  direction was calculated and obtained  $1.89 \text{ \AA}$ . This value of the orthogonal projection was in good agreement with the short (Mg, Nb)-O distance shown in Fig. 4(c). From this fact, it was considered that the decrease of short (Mg, Nb)-O distance caused access of electron cloud and that would give rise to the instability of linear linkage of  $\text{BO}_6$  octahedra then brought about the slight rotation of  $\text{BO}_6$  octahedra to release the instability. This slight rotation would give a chance to form pyrochlore type compound. As shown in Fig. 4(d), the slight rotation of  $\text{BO}_6$  octahedra causes local cutting of the  $\text{BO}_6$  octahedra linkage unaccompanied with topo-chemical reaction and form polycrystal pyrochlore type compound. Actually it was difficult to construct the lattice of pyrochlore type compound after PMN single crystal decomposed at high temperature by using four-circle diffractometer. Figure 5 also shows the change of the orthogonal projection of pyrochlore B-O distance along  $\langle 110 \rangle$  direction. From this figure, it was shown that the decomposition temperature of PMN ( $600^\circ\text{C}$ ) shown in Fig. 1 is in good agreement with the temperature which the short (Mg, Nb)-O distance of PMN coincides with the orthogonal projection of pyrochlore B-O distance along  $\langle 110 \rangle$  direction.

## 5. Conclusions

Crystal structure parameters including  $B$  thermal parameters were determined for  $\text{PbMg}_{1/3}\text{Nb}_{2/3}\text{O}_3$  (PMN) between 27 and  $700^\circ\text{C}$  using a single crystal high temperature X-ray diffraction technique. Several kinds of shift directions for each constituent atom have been reported until now. However, from our refinements, it was clarified that for Pb and (Mg, Nb) atoms the optimum shift directions were not a single direction but "spherical" shifts were plausible, and for O atom the distribution is two parallel rings away from  $XY$  plane. On the basis of this model, the mechanism of thermal decomposition of perovskite PMN into polycrystal pyrochlore type compound was interpreted by the slight rotation of  $\text{BO}_6$  octahedra that was brought about the difference of linear thermal expansion coefficient against Mg-O and Nb-O distances at high temperature.

## References

- 1) L. Börnstein, "Ferroelectrics and Related Substances, New Series", Vol. 16, Springer-Verlag, Berlin, Heidelberg, New York (1981) pp. 389-92.
- 2) B. H. Kim, O. Sakurai and N. Mizutani, Proc. 4th Fall Meeting of the Ceram. Soc. Japan (1991) p. 290.
- 3) H. M. Jang, S. H. Oh and J. H. Moon, *J. Am. Ceram. Soc.*, **75**, 82-88 (1992).
- 4) H. B. Krause, *Acta Cryst.*, **A35**, 1015-17 (1979).
- 5) L. A. Shebanov, P. P. Kapostins and J. A. Zvirgzds, *Ferroelectrics*, **56**, 53-56 (1984).
- 6) E. Husson, M. Chubb and A. Morell, *Mater. Res. Bull.*, **23**, 357-61 (1988).
- 7) J. Chen, H. M. Chan and M. P. Harmer, *J. Am. Ceram. Soc.*,

- 72, 593–98 (1989).
- 8) P. Bonneau, P. Garnier, E. Husson and A. Morell, *Mater. Res. Bull.*, **24**, 201–06 (1989).
  - 9) N. de Mathan, E. Husson, P. Gaucher and A. Morell, *Mater. Res. Bull.*, **25**, 427–34 (1990).
  - 10) N. de Mathan, E. Husson, G. Calvarin, J. R. Gavarri, A. W. Hewat and A. Morell, *J. Phys. Condens. Matter*, **3**, 8159–71 (1991).
  - 11) N. de Mathan, E. Husson, G. Calvarin and A. Morell, *Mater. Res. Bull.*, **26**, 1167–72 (1991).
  - 12) P. Bonneau, P. Garnier, G. Calvarin, E. Husson, J. R. Gavarri, A. W. Hewat and A. Morell, *J. Solid State Chem.*, **91**, 350–61 (1991).
  - 13) N. de Mathan, E. Husson and A. Morell, *Mater. Res. Bull.*, **27**, 867–76 (1992).
  - 14) K. Itoh, L. Z. Zeng, E. Nakamura and N. Mishima, *Ferroelectrics*, **63**, 29–37 (1985).
  - 15) A. Verbaere, Y. Piffard, Z. G. Ye and E. Husson, *Mater. Res. Bull.*, **27**, 1227–34 (1992).
  - 16) Z.-G. Ye, P. Tissot and H. Schmid, *Mater. Res. Bull.*, **25**, 739–48 (1990).
  - 17) N. Wakiya, A. Saiki, N. Ishizawa, K. Shinozaki and N. Mizutani, *Mater. Res. Bull.*, **28**, 137–43 (1993).
  - 18) N. Ishizawa, Y. Yokotani, O. Sakurai and M. Kato, Abstracts Annual Meeting of the Ceram. Soc. Japan (1980) p. 196.
  - 19) T. Sakurai, Universal Program System for Crystallographic Computation, Crystallographic Society of Japan (1967).
  - 20) P. Coppens and W. C. Hamilton, *Acta Cryst.*, **A26**, 71–83 (1970).
  - 21) M. Tokonami, *Acta Cryst.*, **19**, 486 (1965).
  - 22) R. M. Hazen and C. T. Prewitt, *Am. Mineral.*, **62**, 309–15 (1977).